Ceramics International 47 (2021) 4864–4873

Contents lists available at ScienceDirect

Ceramics International

journal homepage: www.elsevier.com/locate/ceramint

Evaluation of locally available amorphous waste materials as a source for alternative alkali activators

Katja König, Katja Traven, Majda Pavlin, Vilma Ducman *

ZAG Ljubljana, Dimičeva 12, 1000, Ljubljana, Slovenia

ARTICLE INFO

Keywords:
Alkali-activated materials
Alternative activators
Waste glass
Waste mineral wool
Cathode-ray tube glass
Solubility

ABSTRACT

The production of alkali-activated materials with excellent mechanical performance requires the use of water glass, which has a significant carbon footprint. Such materials can have a lower carbon footprint if we replace water glass with alternative activators sourced from waste. In this study, we assessed the suitability of locally available amorphous waste materials (stone wool, glass wool, bottle glass and cathode-ray tube glass) as a source for the preparation of alternative alkali activators. We quantified the amount of silicon and aluminium dissolved in the activator solutions via inductively coupled plasma-optical emission spectrometry. The alternative activators were then used to produce alkali-activated fly ash and slag. The compressive strength values of alkali-activated fly ash specimens upon the addition of NaOH, water glass and the most promising alternative activator were 38.98 MPa, 31.34 MPa and 40.37 MPa, respectively. The compressive strength of slag specimens activated with alternative activators with the highest concentration of dissolved silicon (21 g/L) was, however, 70% higher than the compressive strength of slag specimens activated with only 10 M sodium hydroxide. The compressive strength of slag specimens with the addition of the most promising alternative activator was significantly lower (3.5 MPa) than the compressive strength of those that had been activated by commercial water glass (34.3 MPa).

1. Introduction

Alkali-activated materials (AAM) are formed when amorphous aluminosilicate precursors react with alkali activator solutions [1]. The materials most studied as precursors have been natural raw materials (metakaolin), industrial by-products (fly ash and different slags), recycled aluminosilicate sources (glass and mineral wool waste), and combinations thereof [2]. Aqueous solutions of alkali metal hydroxides and silicates (water glass) have usually been used as activators.

Alkali-activated materials have been widely studied over the last decade, as they present a technically acceptable alternative to ceramics or concrete. Moreover, when compared to other technically competitive products, alkali-activated materials have a number of environmental benefits, as has been proven through life cycle assessment (LCA) [3]. Their environmental benefits are particularly apparent if they are produced from locally available waste materials, since they then do not present a burden to the environment [4,5].

There are also, nevertheless, some less favourable calculations with respect to the individual ingredients of alkali activated materials. In particular, the production of water glass requires significant energy, and is responsible for the largest overall contribution to the final carbon footprint of alkali activated materials [6,7]. The cost of such commercial activators is also high when comparing alkali-activated materials to cement-based solutions.

More recently, special attempts have therefore been made to either partially or fully replace water glass in alkali-activated materials. One possibility to achieve this is to reuse glass [8] and mineral wool waste generated at their end-of-life disposal for the production of alkali-activated materials [9]. In this respect, these wastes can be used as 1) precursors for the production of alkali-activated materials or 2) as raw materials for the preparation of alternative activators.

Glass waste has already been used many times as a precursor in alkali-activated materials. Glass is highly amorphous, and has pozzolanic properties. Types of glass which have been successfully used in the production of alkali-activated materials are municipal glass, industrial glass, glass derived from lighting equipment, fluorescent lamps, solar panel waste glass, thin-film transistor liquid display panels, borosilicate glass from pharmaceutical packaging, and glass from the vitrification of

* Corresponding author. ZAG Ljubljana (Slovenian National Building and Civil Engineering Institute), Dimičeva 12, 1000, Ljubljana, Slovenia.
E-mail addresses: vilma.ducman@zag.si, vilma.duman@gmail.com (V. Ducman).
URL: http://www.zag.si (V. Ducman).

https://doi.org/10.1016/j.ceramint.2020.10.059
Received 23 June 2020; Received in revised form 6 October 2020; Accepted 9 October 2020
Available online 9 October 2020

Table 1
Chemical composition of raw materials presented as mass percentages in oxide form (wt. %, XRF) and specific surface area of raw materials. LOI is loss on ignition at 950 °C.

Oxide [wt. %]	waste glassy materials for the preparation of alternative activator solutions				solid precursors	
	Stone wool (SW)	glass wool (GW)	bottle glass (BG)	CRT glass (CRTG)	fly ash (FA)	slag (SLAG)
LOI (950˚C)	/	/	/	/	0.51	14.31
Na_2O	3.85	15.31	13.47	7.61	1.19	0.13
MgO	11.70	4.10	1.68	0.46	2.80	14.87
Al_2O_3	16.09	3.11	0.91	2.07	22.98	8.54
SiO_2	43.60	65.44	72.37	58.49	44.82	21.05
K_2O	0.57	0.85	0.73	7.35	2.20	0.17
CaO	16.77	8.99	10.07	1.15	12.38	20.87
Fe_2O_3	5.34	0.73	0.21	0.16	10.65	11.37
BaO	/	0.05	0.07	7.72	0.08	0.017
PbO	/	/	0.06	3.92	/	0.017
BET surface area [m^2/g]	0.37	0.44	0.45	0.53	2.85	7.61

municipal residues [10].

Due to its high alkali and silica content, recycled glass used as a precursor in combination with potassium and sodium hydroxide solutions has been shown to be an adequate substitute for water glass in the synthesis of alkali-activated materials in certain situations. In this instance a silicate activator is not needed to achieve high compressive strength, thus noticeably lowering the cost of production [11–13]. In one study, for example, green soda-lime-silica waste glass with a high content of silica (ca. 72%) was utilised as a precursor and activated by alkali hydroxide solutions. The resulting alkali-activated material had a compressive strength of up to 60 MPa after 56 days of curing [11]. In another case, mechanical strength of 30 MPa was achieved by using only recycled glass as a precursor, but the material was not hydrolytically stable, thus severely reducing strength in moist conditions [10].

Recycled glass cannot be used alone in the processing of alkali-activated materials, because it does not provide a suitable SiO_2/Al_2O_3 molar ratio. It can, however, still be used in addition to other solid aluminosilicate sources. As the amount of glass in the alkali-activated product increases, the degree of polymerisation decreases, and consequently negatively impact the mechanical properties [10,14,15]. In a comparative study where glass powder, fly ash and mixtures of these two materials were activated, it was found that the glass powder-based activated cements developed higher strengths than activated fly ash cements, when each of which were solidified at room temperature. For structure stabilisation, tetrahedral aluminium had to be introduced, i.e. glass was mixed with fly-ash to increase the usually low content of alumina in the waste glass. A source of calcium can also be added to create an insoluble gel [16]. When boron-silicate glass was used as a precursor together with fly ash, boron was proven to be in the inorganic polymeric chain, where it partially replaced aluminium [10,17].

Mineral wool waste has also been used as a precursor in alkali activation [18–21]. The chemical composition of stone wool and glass wool differs, with glass wool with an SiO_2 content of 60–65 wt % falling into the compositional region of soda-lime silicate glasses such as glass waste, whereas stone wool is closer to ground granulated blast furnace slag. However, ground granulated blast furnace slag contains more calcium and less magnesium than stone wool [22].

To date, there have been no publications using mineral wool waste for the preparation of alkali activators. On the contrary, glass waste has already been utilised successfully as a raw material for producing cost-effective sodium silicate solutions to be used as alternative alkali activators [23,24]. Urban waste glass has been used for the production of sodium silicate solutions with "dissolution" in sodium hydroxide/sodium carbonate solutions [25]. These solutions were used as an alkali activator for synthesising cements based on alkali-activated slag [13] and alkali-activated fly ash, yielding compressive strengths similar to those obtained when using commercial sodium silicates (water glass) [26].

Bouchikhi et al. tested the residual waste from recycled glass as an alternative activator in a metakaolin based geopolymer matrix. Among three treatment programs used, treatment in highly alkaline media (10 M NaOH) at an elevated temperature (90 °C) resulted in leachates with the highest quantity of silica. Furthermore, the mechanical properties of the geopolymers produced with this alternative activator were 2.3-times higher than the mechanical properties of geopolymers activated with only 10 M NaOH [27].

Keawthun et al. studied hydrothermal and fusion methods to prepare a sodium silicate solution from waste glasses of three different colours. The hydrothermal method was more promising for bottle waste glass of all colours due to a better Na_2O/SiO_2 molar ratio (white bottle glass exhibited the best performance, t. i. $Na_2O/SiO_2 = 1/7.74$). Nevertheless, 60 min of alkaline fusion treatment at 650 °C with 90 wt % of NaOH also resulted in an appropriate composition of liquid sodium silicate composition [28]. The potential of the solution for alkali activation depends on the type of glass, time, temperature, size of the glass particles and the pH of the solution during preparation. Pastes composed of blast furnace slag and an activator based on waste glass and sodium hydroxide/sodium carbonate had similar rheological properties to pastes composed of blast furnace slag and commercial water glass. Alkali-activated slag materials using waste glass as an activator showed high performance, durability, and shear stress stability.

Alternative alkali activators derived from rice husk ash have also been proven as an effective substitute for commercial sodium silicate in the production of alkali-activated materials based on fly ash and ground granulated blast furnace slag [29]. Similarly, activators produced from rice husk ash have been successfully applied in the production of metakaolin based geopolymers [30,31].

The goal of the present research was to evaluate the suitability of various waste glassy materials mixed with sodium hydroxide as alternative activators in the preparation of alkali-activated materials. Four locally-available materials were selected for the study: waste bottle glass, waste glass wool, waste stone wool and cathode-ray tube glass.

2. Experimental

2.1. Raw materials for the preparation of alternative activators

Four different waste materials were obtained from a waste disposal centre for the preparation of alkali activators; glass wool (GW), stone wool (SW), bottle glass (BG) and cathode-ray tube glass (CRTG). Both types of mineral wool were milled, homogenised and dried in a drying oven at 105 °C for 24 h and then sieved to a particle size below 63 μm. Bottle glass and cathode-ray tube glass were milled, homogenised and sieved to a particle size below 90 μm.

2.2. Precursors for the preparation of alkali-activated materials

Fly ash from a thermal power plant and electric arc furnace slag from the metallurgical industry in Slovenia were used as precursors for the preparation of alkali-activated materials. Fly ash was used as received, whereas slag was milled, homogenised and sieved to a particle size below 90 μm.

2.3. Characterization of raw materials

The chemical composition of the raw materials was determined by a sequential X-Ray fluorescence (XRF) spectrometer (ARL PERFORM'X, Thermo Fisher Scientific Inc., USA) using UniQuant software. Before measurement, the powder samples were heated to 950 °C and then fused

Table 2
The paste formulations presented as mass percentages of the precursors and activators (wt. %), nominal Si/Al molar ratio and Na/Al molar ratio.

	Precursor (wt. %)	Activator (wt. %)	Si/Al	Na/Al
SWA-4h-FA	78.8	21.2	1.4/1	0.4/1
SWA-24h-FA	78.8	21.2	1.4/1	0.4/1
GWA-4h-FA	78.8	21.2	1.4/1	0.4/1
GWA-24h-FA	78.8	21.2	1.4/1	0.4/1
BGA-4h-FA	78.8	21.2	1.4/1	0.4/1
BGA-24h-FA	78.8	21.2	1.4/1	0.4/1
CRTGA-4h-FA	78.8	21.2	1.4/1	0.4/1
CRTGA-24h-FA	78.8	21.2	1.4/1	0.4/1
Ref 10 M NaOH-FA	78.8	21.2	1.4/1	0.4/1
Ref-Water glass-FA	71.9	28.1	1.7/1	0.4/1
SWA 4h-SLAG	67.0	33.0	1.6/1	2.4/1
SWA 24h-SLAG	67.0	33.0	1.6/1	2.4/1
GWA 4h-SLAG	67.0	33.0	1.7/1	2.4/1
GWA 24h-SLAG	67.0	33.0	1.6/1	2.4/1
BGA 4h-SLAG	67.0	33.0	1.6/1	2.4/1
BGA 24h-SLAG	67.0	33.0	1.7/1	2.4/1
CRTGA 4h-SLAG	67.0	33.0	1.6/1	2.4/1
CRTGA 24 h-SLAG	67.0	33.0	1.6/1	2.4/1
Ref-10 M NaOH-SLAG	67.0	33.0	1.5/1	2.4/1
Ref-Water glass-SLAG	68.8	31.2	3.0/1	1.6/1

beads were prepared at 1050 °C–1100 °C using commercially available flux composed of 50% lithium tetraborate and 50% lithium metaborate (FX-X50-2, Fluxana GmbH & Co. KG, Germany). The mass ratio of powder to flux was 1:10.

Nitrogen sorption at a temperature of 77 K (ASAP 2020, Micromeritics, Norcross, USA), in the relative pressure range between 0.05 and 0.3, was used to determine the specific surface area of the powders. Before each measurement the powders were heated to 70 °C–105 °C for at least 3 h and degassed to 10^{-3} Torr (Flowprep equipment, Micromeritics, Norcross, GA, USA). The specific surface area was calculated using the Brunauer–Emmett–Teller (BET) method.

The chemical compositions and BET surface areas of the raw materials are shown in Table 1. The initial waste materials for the preparation of alternative activators contained differing amounts of SiO_2. Bottle glass contained the highest amount of SiO_2 (72.4 wt %), while glass wool contained 65.4 wt % SiO_2, cathode-ray tube glass 58.5 wt % SiO_2, and the stone wool contained the lowest amount of SiO_2 (43.6 wt %). Stone wool contained the highest amount of Al_2O_3 (16.1 wt %), while the other waste glasses contained between 1-3 wt %. All four milled and sieved waste glassy powders had BET specific surface areas between 0.37 m^2/g and 0.53 m^2/g.

The precursors also contained different amounts of SiO_2 and Al_2O_3. Fly ash contained 44.8 wt % SiO_2 and 23.0 wt % Al_2O_3, while slag contained only 16.8 wt % SiO_2 and 8.1 wt % Al_2O_3. Slag had higher contents of CaO (21.4 wt %) and MgO (16.8 wt %). The specific surface area of fly ash and slag was 2.85 m^2/g and 7.61 m^2/g, respectively. The mass percentage of amorphous phase in fly ash and slag has previously been reported as 78.7% [32] and 63.2% [33], respectively.

2.4. Preparation and characterization of alternative alkali activators

Either 5 g or 20 g of the glassy waste powders were added to 200 mL of 10 M sodium hydroxide solution, resulting in ratios of powder mass to volume of 10 M NaOH (m_{powder}/V_{NaOH}) of 0.025 g/mL and 0.1 g/mL, respectively. The 10 M NaOH solution was prepared in the laboratory from distilled water and NaOH flakes (Donau Chemie AG, Austria). The suspensions were left boiling at 120 °C for either 4 h or 24 h while subject to constant mixing with a magnetic stirrer at 400 rpm. The suspensions were then cooled and filtered through a cellulose filter with a retention capacity of 4 μm–12 μm (MN 640 m, (Macherey-Nagel GmbH & Co. KG, Germany). The filtrates obtained were analysed by inductively coupled plasma-optical emission spectrometry (ICP-OES; Varian, Model 715-ES) in order to determine their silicon and aluminium content and then later used as alternative activator solutions.

2.5. Preparation and characterization of alkali-activated materials

In order to evaluate their effectiveness, the alkali activator solutions prepared were used for the alkali activation of 1) fly ash and 2) slag precursors. The pastes of the precursors and alternative activators were prepared at a constant mass ratio of alternative activator to the precursor. The paste formulations, presented as mass percentages of the precursors and activators (wt. %), nominal Si/Al molar ratio, and Na/Al molar ratio, are reported in Table 2.

The mass of the fly ash m(FA) was 150.0 g. For the mixtures with fly ash, the mass of the alternative activators m(AA) was 40.4 g, giving a mass ratio m(AA)/m(FA) of 0.27. Two reference specimens were prepared with fly ash: a) 150.0 g fly ash mixed with 40.4 g of 10 M NaOH (m(NaOH)/m(FA) = 0.27) and b) 150.0 g fly ash mixed with 58.5 g of water glass (WG), (m(WG)/m(FA) = 0.39). The mass of the slag m(slag) was 150.0 g. For the mixtures with slag, the mass of the alternative activators was 74.0 g, giving a mass ratio m(AA)/m(slag) of 0.49. Two reference specimens were prepared with slag: a) 150.0 g of slag mixed with 74.0 g of 10 M NaOH (m(NaOH)/m(FA) = 0.49) and b) 150.0 g of slag mixed with 68.1 g of water glass (m(WG)/m(FA) = 0.45). As a reference alkali activator, commercially available sodium silicate solution, water glass (Na_2O; 15.4%, SiO_2; 30.4%, H_2O; 54.2%), was used (Crystal 0112, Tennants Distribution Ltd, United Kingdom).

The pastes were mixed manually for 2 min and then cast into silicon rubber moulds of dimensions 80 x 20 x 20 mm^3. In the unsealed moulds, the pastes were then put in a heating chamber in a natural atmosphere for 72 h at a temperature of 70 °C in order to accelerate the alkali-activation process and thus harden the structure. The hardened binders were then demoulded and their mechanical strength was measured. The mechanical strength (compressive and bending strength) was determined using a compressive and bending strength testing machine (ToniTechnik ToniNORM, Berlin, Germany) at a force application rate 0.05 kN/s. The bending strength of the specimens was assessed using the three-point bending test/method, and the compressive strength was assessed using the two broken portions from the bending test. The reported bending strength values represent the average results obtained from 3 test specimens of dimensions (20 × 20 × 80) mm^3. The reported compressive strength values represent the average results obtained from 5 test specimens.

The porosity of the hardened binders was analysed using a mercury-intrusion porosimeter (AutoPore IV 9500, Micromeritics, Norcross, USA) in the pressure range 0.004 MPa–414 MPa. Before the measurement, representative fragments of the alkali-activated materials with a volume of approximately 1 cm^3 were dried in a heat chamber at 70 °C for 24 h.

Infrared spectra of the raw precursors and hardened binders were recorded using a Fourier transform infrared (FTIR) spectrometer

Table 3
The concentration of silicon [g/L] and aluminium [mg/L] in the alternative activators under different dissolution conditions. The numbers in brackets represent the dissolution efficiency of silicon and aluminium as percentages. The dissolution efficiency was calculated from XRF and ICP-OES results.

dissolution conditions		SW activator (SWA)		GW activator (GWA)		BG activator (BGA)		CRTG activator (CRTGA)	
Boiling time [h]	m_{powder}/V_{NaOH} [g/mL]	c(Si) [g/L]	c(Al) [mg/L]	c(Si) [g/L]	c(Al) [mg/L]	c(Si) [g/L]	c(Al) [mg/L]	c(Si) [g/L]	c(Al) [mg/L]
4	0.025	4 (77)	1334 (61)	6 (77)	310 (74)	/	/	/	/
	0.1	5 (24)	730 (8)	18 (58)	547 (33)	11 (32)	213 (43)	5 (18)	214 (19)
24	0.025	5 (95)	701 (32)	6 (77)	326 (78)	/	/	/	/
	0.1	7 (34)	362 (4)	11 (35)	232 (14)	21 (61)	418 (85)	11 (39)	433 (39)

Table 4
Density, porosity and mechanical strength of the hardened binders prepared by alkali-activation of fly ash using various alternative activators, after curing for 72 h at 70 °C. Standard deviations for the compressive and bending strength are shown in parentheses.

Specimen name	The molar ratio Na/Al/Si in the formulations	Density [g/cm^3]	Open porosity [%]	Total pore area [m^2/g]	Compressive strength [MPa]	Bending strength [MPa]
SWA-4h-FA	0.4/1/1.4	1.67	15.63	15.628	40.37 (7.42)	9.78 (0.51)
SWA-24h-FA	0.4/1/1.4	1.65	27.40	17.360	38.28 (3.81)	10.16 (1.5)
GWA-4h-FA	0.4/1/1.4	1.75	21.18	21.176	31.02 (7.44)	6.14 (0.69)
GWA-24h-FA	0.4/1/1.4	1.76	32.61	23.261	30.95 (3.28)	5.88 (1.66)
BGA-4h-FA	0.4/1/1.4	1.64	21.14	21.136	23.86 (1.86)	6.11 (1.70)
BGA-24h-FA	0.4/1/1.4	1.67	27.81	19.041	31.31 (2.81)	7.39 (0.60)
CRTGA-4h-FA	0.4/1/1.4	1.67	28.06	21.835	33.36 (7.24)	8.16 (1.16)
CRTGA-24h-FA	0.4/1/1.4	1.63	30.82	22.597	32.97 (7.99)	3.78 (0.25)
Ref 10 M NaOH-FA	0.4/1/1.4	1.67	30.67	21.828	38.98 (7.55)	9.16 (0.32)
Ref-Water glass-FA	0.4/1/1.7	1.74	26.56	2.546	31.34 (3.86)	9.08 (1.49)

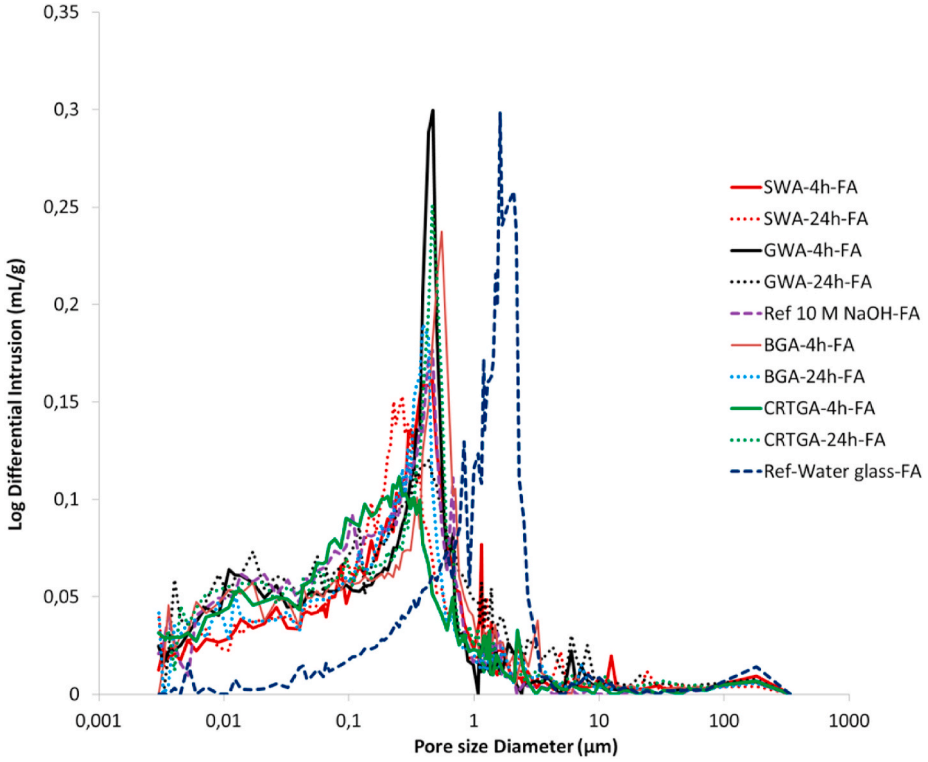

Fig. 1. Pore size distribution of the hardened binders composed of alkali-activated fly ash, after curing at 70 °C for 72 h.

(Spectrum Two, PerkinElmer, USA) equipped with an attenuated total reflection accessory (Universal ATR) with a diamond/ZnSe crystal as a solid sample support in the range from 450 cm^{-1}–4000 cm^{-1} and with a resolution of 1 cm^{-1}. The precursors were analysed as they were prepared for the alkali-activation process, whereas the hardened binders were ground before the analysis.

The microstructures of the hardened binders were observed at polished cross-sections in a scanning electron microscope (SEM; JEOL JSM-IT500 LV, Tokyo, Japan). The SEM was equipped with an energy-dispersive X-ray spectrometer (EDS, Oxford Instruments) coupled with Aztec software for the quantitative analyses of elemental compositions. Before SEM scanning, the specimens were vacuum-dried at 40 °C in a vacuum drier.

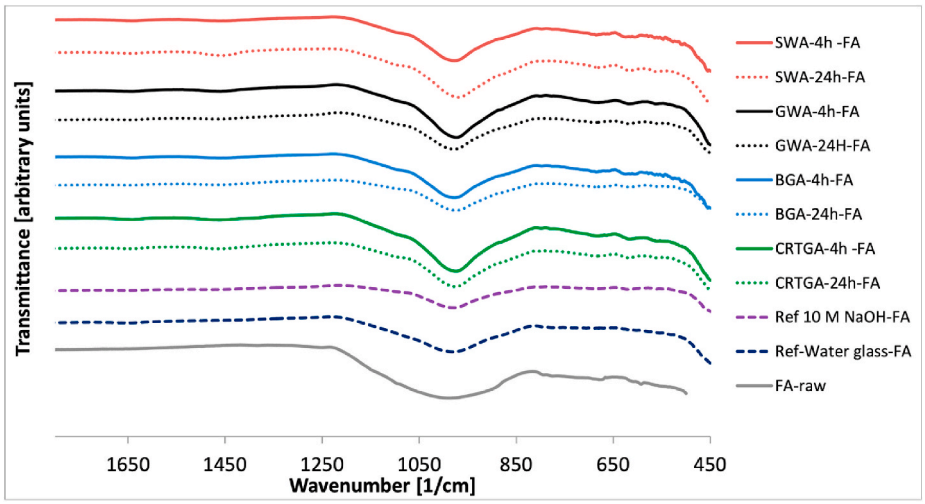

Fig. 2. Infrared spectra (transmittance) of the hardened binders composed of alkali-activated fly ash after curing at 70 °C for 72 h.

3. Results and discussion

3.1. The concentration of dissolved silicon and aluminium in the alternative alkali activators

Table 3 shows the concentration of dissolved silicon and aluminium in the prepared alternative alkali activators based on stone wool (SWA), glass wool (GWA), bottle glass (BGA) and cathode-ray tube glass (CRTGA), as determined by ICP-OES analysis. As the amount of SW powder in the starting suspension (m_{powder}/V_{NaOH}) increased, there was a slight increase in the concentration of silicon in the SWA solution, but the dissolution efficiency of the silicon decreased at both dissolution times studied (4 h and 24 h). As the amount of SW powder in the starting suspension increased, both the concentration of aluminium and the dissolution efficiency for the SWA solution decreased. As the amount of GW powder in the starting suspension increased, the concentration of dissolved silicon in the GWA solution increased dramatically, but the dissolution efficiency of silicon decreased, at both dissolution times studied (4 h and 24 h). As the amount of GW powder increased, the concentration of aluminium in the GWA solution increased when the dissolution duration was 4 h and decreased when the dissolution time was 24 h. Nevertheless, in both cases, the dissolution efficiency of aluminium in the GW powder decreased.

In the case of SW, with a constant quantity of powder in the starting suspension, the concentration and dissolution efficiency of silicon slightly increased as the dissolution time increased. On the contrary, the concentration and dissolution efficiency of aluminium decreased with a longer dissolution time. When a low amount of GW powder was used in the starting suspension ($m_{powder}/V_{NaOH} = 0.025$ g/mL), the concentration and dissolution efficiency of silicon and aluminium remained almost unchanged with a greater dissolution time. When a higher amount of GW powder was used in the starting suspension ($m_{powder}/V_{NaOH} = 0.1$ g/mL), the longer dissolution time decreased the dissolution efficiency of both silicon and aluminium.

The waste bottle glass had a higher amount of silicon and slightly less aluminium than glass wool, while the quantities of both silicon and aluminium were lower in the cathode-ray tube glass compared to glass wool (Table 1). In contrast to the mineral wool activators, the concentrations and dissolution efficiencies of silicon and aluminium increased with a prolonged dissolution time in the case of both waste glass activators.

Si–O–Si bonds are stronger than those of Si–O–Al and Al–O–Al [34]. Alkali dissolution/precipitation reactions are controlled by the Si-rich, Al-deficient surface precursor species at the mineral surface. Al preferentially dissolves from aluminosilicate glasses and minerals by Al-proton exchange reactions, which results in a Al-deficient layer on the surface. Silicon that had previously bonded to the aluminium then becomes exposed, and the liberated silicon dissolves [35].

Due to weaker nature of the Al–O bonds, and the higher concentration of aluminium in the SW powder, a higher concentration of aluminium in the solution was expected. This was partly true at a lower m_{powder}/V_{NaOH} ratio, after 4 h of boiling. The concentration of aluminium halved after 24 h of boiling at the same m_{powder}/V_{NaOH} ratio. A similar trend was observed when a higher amount of stone wool was added to the NaOH solution, as well as with glass wool at a higher m_{powder}/V_{NaOH} ratio. The phenomena of decreasing silicon and aluminium concentrations in the glass and stone wool solutions when a higher amount of precursor and/or longer dissolution time applied could be explained by the formation of various solid species. A disordered phase could be present at relatively high supersaturation [36], which may precipitate at different equilibrium Al/Si ratios [37]. A decrease in Al and/or Si concentration may also be related to the accumulation of ions on the surface which disable or slow down the dissolution process. Due to readsorption and formation of different unstable complexes (condensation process), ionised silanol group Si–O- on the surface attracts cations, which provide a barrier for further dissolution [38].

It follows that in alternative activators made of stone and glass wool a longer dissolution time does not provide a significantly higher amount of silicon and aluminium compared to alternative activators made of cathode-ray tube and waste bottle glass. It is proposed that after a certain period of time the dissolution of silicon and aluminium reach steady-state conditions. Since glass wool has a similar chemical composition to waste cathode-ray tube and bottle glass, additional studies are needed to evaluate the effect of other ions on the dissolution process, as well as the possible formation of precipitation. The silicon concentrations in the alternative activator based on bottle glass (11 g/L after 4 h and 21 g/L after 24 h of dissolution) are in good agreement with previous studies performed on the dissolution of waste glass in highly alkaline media [13,27,39]. When Puertas et al. used 0.1 g/mL and 0.25 g/mL of waste glass powder of particle size 45 μm and heated it in a $NaOH/Na_2CO_3$ solution for 6 h at 85 °C, the concentrations of SiO_2 were 2.83 g/100 mL (13.16 g Si/L) and 4.54 g/100 mL (21.23 g Si/L), respectively. Moreover, temperature is a crucial variable in the solubilisation of glass. When SiO_2 was dissolved at 80 °C and 50 °C, for both 6 h and 24 h, the highest amount of SiO_2 was leached when the highest temperature was applied for the longest dissolution time, i.e. 80 °C for 24 h.

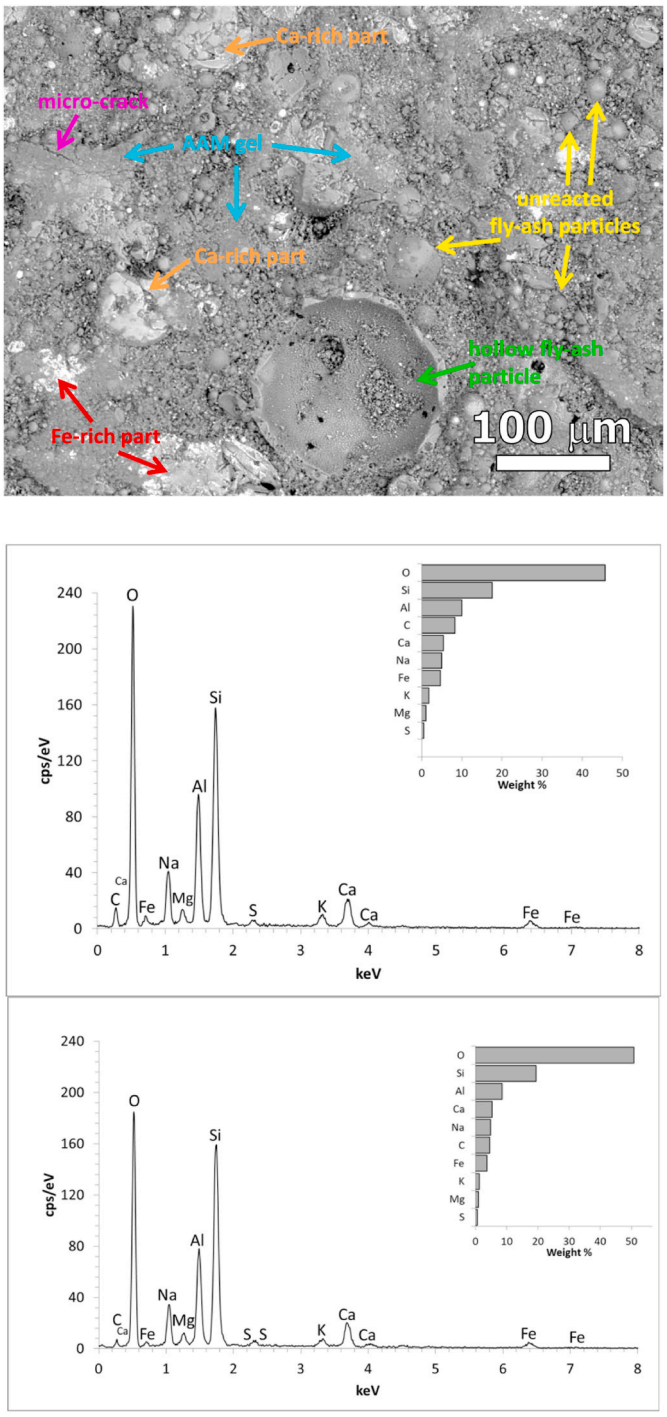

Fig. 3. (a) SEM micrograph of SWA-4H.FA, b), EDS spectrum of SWA-4H-FA and c) EDS spectrum of Ref-Water glass-FA specimens.

3.2. Mixtures of the alternative activators with fly ash

In the next step, the alkali-activated materials were prepared by mixing fly ash with the activators obtained by dissolution of waste powders in 10 M NaOH at a m_{powder}/V_{NaOH} ratio of 0.1 g/mL, while maintaining a fixed mass ratio of activator solution to precursor and the same curing regime. Table 4 summarises the density, porosity and mechanical strength of the hardened binders. The Na/Al ratio of 0.4 was equal in all mixtures, while the Si/Al ratio was 1.4 in all mixtures except the one containing water glass, in which it was 1.7. It should be noted that these numbers indicate the ratio of elements in the whole mixture and not only in the formed gel.

Table 4 shows the a) compressive strength, and b) bending strength of hardened fly ash specimens synthesised from alternative activators and 10 M sodium hydroxide. It is clear that the specimen produced from BGA (silicon concentration of 11 g/L, aluminium 213 mg/L) has the lowest compressive strength, while the specimen produced from CRTGA (silicon concentration of 11 g/L, aluminium 433 mg/L) exhibits the lowest bending strength. In contrast, specimens prepared by sodium hydroxide (Ref. 10 M NaOH-FA) and SW activators (silicon concentrations of 5 g/L and 7 g/L) exhibit the highest levels of compressive (~ 40 MPa) and bending (~ 10 MPa) strength. Fly-ash specimens produced from activators with the highest concentration of dissolved silicon (GWA; 18 g Si/L and BGA; 21 g Si/L) exhibit solid mechanical properties. It is clear that the silicon concentration in the activators did not obviously impact the mechanical strength of the fly-ash specimens. For this reason, evaluation of the effectiveness of alternative activators in the fly ash specimens is not sufficient. Namely, a high inherent content of amorphous silicon and aluminium in the fly ash makes it possible to achieve good mechanical strength of the alkali-activated specimens only by the addition of 10 M sodium hydroxide. It is essential to use a long enough curing time for fly ash particles to be sufficiently bonded [40].

Fig. 1 shows the pore size distribution of solid binders composed of alkali-activated fly ash. Pore size is approximately the same in almost all specimens except the fly ash specimen activated with water glass, which has slightly larger pores. Since the total pore area is inversely proportional to the pore diameter, the total pore area of the fly ash specimen activated with water glass is much lower than in the other specimens (Table 4). It can be seen in Table 4 that the open porosity of the specimens ranges between 16% and 33%. Since the density of the specimens is similar (from 1.63 g/cm^3 to 1.76 g/cm^3), the difference in open porosity values could be attributed to closed porosity, which could not be detected by mercury intrusion porosimetry.

The process of alkali-activation was further assessed via infrared spectroscopy (FTIR), through which solidified binders, as well as both precursors, were analysed. In the IR spectrum of the unreacted fly-ash precursor, the Si–O-T (T = Si or Al) asymmetric stretching vibration band is present at 992 cm^{-1}, as shown in Fig. 2. This main band shifts to lower values when the alkali-activation process is introduced and is quite similar in all the spectra of the final alkali-activated binders (between 974 cm^{-1} and 980 cm^{-1}), since inherently there is already a sufficient amount of amorphous Si in the precursor. Silicon coming from the alternative activators is therefore not the principal factor influencing the band shift in the IR spectra.

Scanning Electron Microscopy (SEM) with energy-dispersive X-ray spectroscopy (EDS) provided useful information regarding the microstructure and elemental composition of the specimens. In the case of the fly-ash-based alkali-activated materials, a similar pattern was observed in all specimens. A representative micrograph of the SWA-4H-FA specimen is presented in Fig. 3a. Besides AAM gel, which constitutes a major part of the surface (see Fig. 3a, blue arrows), there are also numerous unreacted fly-ash particles (see Fig. 3a, yellow arrows). The particles are generally spherically shaped with a diameter ranging between 1 and 100 µm. Some hollow fly-ash particles are also visible (see Fig. 3a, green arrow). Calcium-rich parts also exist (see Fig. 3a, orange arrows), where the formation of C(A)SH gel is also possible. Fe-rich parts are marked with red arrows, while micro-cracks generated in the AAM gel are marked with purple arrows (Fig. 3a). The molar ratio of Na/Al/Si was confirmed via EDS analysis of the AAM gel (Fig. 3b and c), which complies with the calculations based on the XRF measurements (Table 1).

3.3. Mixtures of the alternative activators with slag

The alternative activators obtained in the dissolution of waste powders in 10 M NaOH at m_{powder}/V_{NaOH} ratio of 0.1 g/mL were mixed with slag while maintaining a fixed mass ratio of the activator solution

Table 5
The molar ratio of Na/Al/Si in the prepared mixtures and the density, porosity and mechanical strength of the hardened slag binders.

Specimen name	The molar ratio Na/Al/Si in the formulations	Density [g/cm^3]	Open porosity [%]	Total pore area [m^2/g]	Compressive strength [MPa]	Bending strength [MPa]
SWA 4h-SLAG	2.4/1/1.6	1.69	42.16	7.896	2.11 (0.08)	0.75 (0.38)
SWA 24h-SLAG	2.4/1/1.6	1.76	41.11	6.851	2.31 (0.18)	0.43 (0.58)
GWA 4h-SLAG	2.4/1/1.7	1.80	40.63	6.386	3.38 (0.31)	1.32 (0.23)
GWA 24h-SLAG	2.4/1/1.6	1.77	40.55	6.883	3.35 (0.18)	0.59 (0.84)
BGA 4h-SLAG	2.4/1/1.6	1.76	40.47	11.350	3.03 (0.37)	1.76 (0.18)
BGA 24h-SLAG	2.4/1/1.7	1.82	39.68	6.216	3.47 (0.12)	1.65 (0.04)
CRTGA 4h-SLAG	2.4/1/1.6	1.67	43.47	10.991	2.09 (0.29)	0.47 (0.62)
CRTGA 24 h-SLAG	2.4/1/1.6	1.71	42.26	9.079	2.92 (0.54)	1.53 (0.02)
Ref-10 M NaOH-SLAG	2.4/1/1.5	1.63	41.34	7.545	2.01 (0.21)	1.07 (0.10)
Ref-Water glass-SLAG	1.6/1/3.0	1.90	24.81	1.850	34.28 (4.03)	7.94 (0.19)

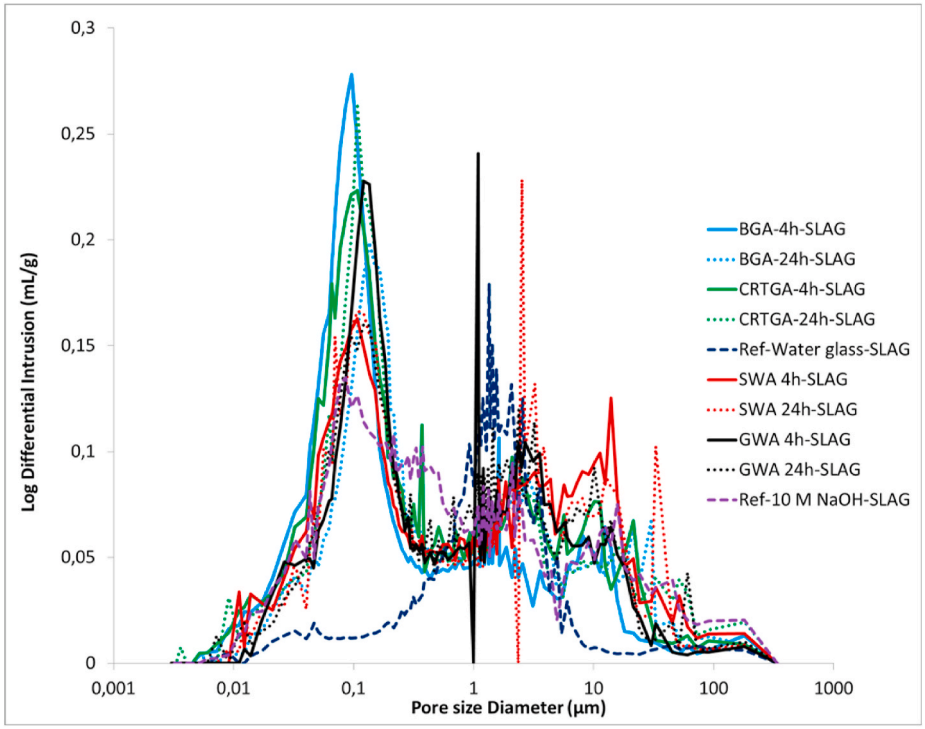

Fig. 4. Pore size distribution of the hardened binders composed of alkali-activated slag after curing at 70 °C for 72 h.

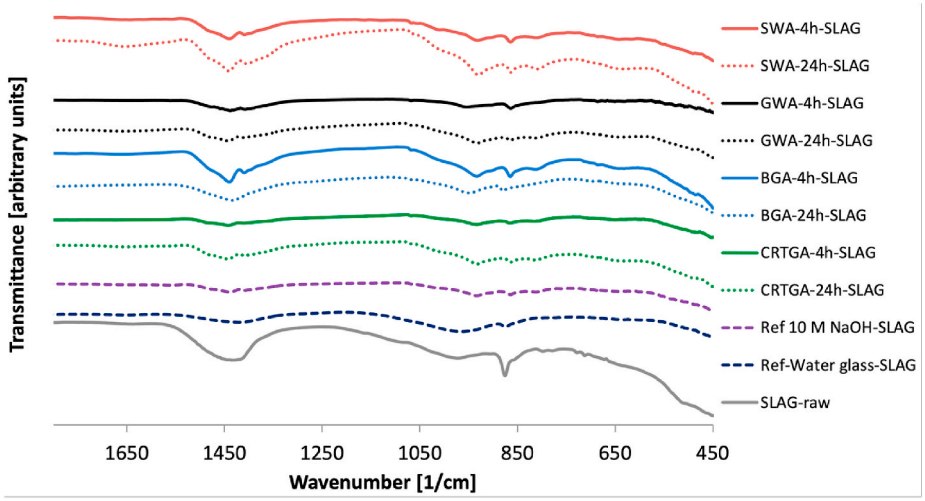

Fig. 5. Infrared spectra (transmittance) of the solid binders composed of alkali-activated slag after curing at 70 °C for 72 h.

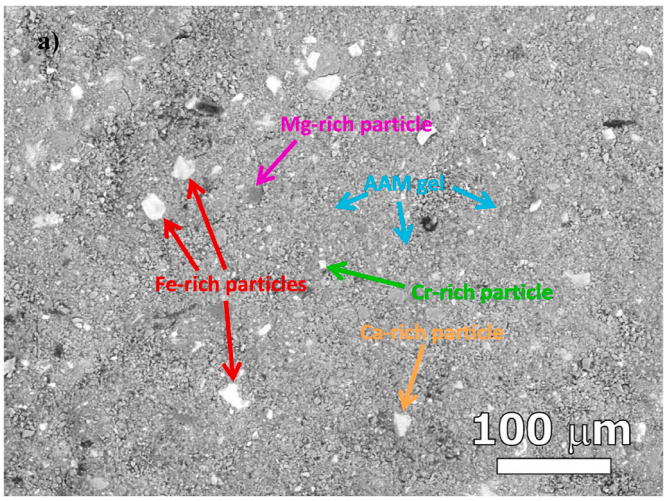

Fig. 6. SEM micrograph of GWA-4H-SLAG.

to the precursor and the same curing regime. Table 5 summarises the calculated molar Na/Al/Si ratios in the prepared reaction mixtures and the density, porosity and mechanical strength of the hardened binders. The Na/Al and Si/Al ratios in all the mixtures were 2.4 and 1.6, respectively, except in the slag mixture with water glass where the Na/Al and Si/Al ratios were 1.6 and 3.0, respectively.

It can be seen in Table 5 that the sample produced from the NaOH solution has the lowest compressive strength. In contrast, when alternative activators were added to slag, a difference in the mechanical strength of hardened specimens was observed. The specimens produced from BGA (silicon concentration of 21 g/L) and GWA (silicon concentrations of 11 g/L and 18 g/L) have the highest compressive strength. Table 5 also shows the bending strength of the hardened slag specimens prepared with alternative activators. The specimens produced from SWA (silicon concentration of 7 g/L) and CRTGA (silicon concentration of 5 g/L) have the lowest bending strength. In contrast, the specimen produced from BGA has the highest bending strength. Given that the slag contains less amorphous phase compared to the fly ash, the amount of silicon in the alternative activators used for the alkali activation of slag is critically important to increase the mechanical strength of hardened slag specimens. With less silicon available for a given reaction, the resulting compressive and bending strength automatically decreased.

Fig. 4 shows the pore size distribution of the solid binders composed of alkali-activated slag. The pore sizes of the specimens prepared with alternative activators are of a similar size to those prepared with 10 M NaOH, with intrusion peaks at approximately 0.1 µm and some pores larger than 10 µm. It can be seen in Table 5 that the open porosity of the specimens ranges between 25% and 44%. The lowest open porosity was shown in the slag specimen activated by water glass.

In this case an Si–O-T asymmetric stretching vibration band is visible in the IR spectra of raw slag at a lower value (973 cm^{-1}) than in the case of raw fly ash. In the case of slag, a major band is also observed at 1435 cm^{-1}, corresponding to the vibrating modes of CO_3 (contained in $CaCO_3$), as well as a sharp peak at 875 cm^{-1}, which corresponds to the carbonation band. The band of main interest (the Si–O-T asymmetric stretching vibration band) also shifts to lower values when the alkali-activation process is introduced (Fig. 5), with the difference between the values of the highest and lowest bands being much more apparent in the case of slag-based alkali-activated materials. The highest band value of 967 cm^{-1} is therefore attributed to the mixture, where also the highest amount of Si is added to the process (mixture Ref-Water glass-SLAG) when commercially available activator was used. In the case when a higher amount of Si is added among alternative activators (GWA-4h and BGA 24h–18 and 21 g/L, respectively), the values shift to 953 and 951 cm^{-1}, respectively. In all other mixtures, the band value is the lowest where the concentration of Si added was 11 g/L or less, falling at around 930 cm^{-1}. From the results above, we can conclude that in the case of slag-based alkali-activated materials, where there is not a sufficient amount of Si present in the raw precursor, the Si coming from the alternative activator is the dominant factor influencing the band shift in IR spectra as well as the mechanical strength of the hardened structures. Additionally, we can further conclude that the assessment of the suitability of alternative activators is more precise when Si-deficient materials are used as precursors. The suitability is then closely dependent on the amount of Si present in the alternative activator and can also be monitored by FTIR spectroscopy.

A similar pattern was observed in the SEM micrographs of all specimens of the slag based alkali-activated materials. A representative micrograph of the GWA-4H-SLAG specimen is presented in Fig. 6. Besides AAM gel, which constitutes a major part of the surface (see Fig. 6, blue arrows), there are numerous unreacted particles from the precursor, which have crystalline nature and are thus unreactive in the alkali-activation process: calcium-rich, iron-rich, chromium-rich parts as well as magnesium-rich particles (Fig. 6). The most significant difference among specimens was observed between the EDS analysis of the AAM gel matrix in the reference specimen Ref-Water glass-SLAG and the other specimens. There is an undeniable difference in the molar ratio of Na/Al/Si, which is favourable in the case of the Ref-Water glass-SLAG specimen (1.63/1/3.00; see Fig. 7b). The sodium content in relation to silicon is much higher in other specimens (2.43/1/1.68; see Fig. 7a), however, which is further reflected in the weak mechanical strength of these specimens.

4. Conclusion

Waste stone wool, glass wool, bottle glass and cathode-ray tube glass were exposed to a leaching process in an NaOH solution in order to develop an alternative activator which could replace commercial sodium silicate. After leaching in 10 M NaOH at different ratios of powder mass to liquid volume and at different dissolution times, the amount of Si and Al released in the filtrates was determined by ICP-OES. Prepared solutions were then further used for the preparation of alkali-activated specimens from two different precursors, fly ash and slag. The mechanical strength of fly ash-based mixtures with each of the alternative activators were compared to a blank sample, where only 10 M NaOH was used, and only in the case of the stone wool activator was a slight increase in mechanical properties observed (app. 3.9% for bending strength and 3.6% for compressive strength). When each of these activators were applied to the slag precursor, whose blank sample mechanical properties are much lower than the one from fly ash (slag contains just over a third of Al and Si than fly ash), the greatest increase in mechanical properties was observed in the case of the activators based on waste bottle glass and waste glass wool; the release of Si was also the highest in these specimens. When the mechanical strength of the slag-based mixtures with each of the alternative activators were compared to the blank sample, where only 10 M NaOH was used, an increase in mechanical properties was observed when activators from waste bottle glass and waste glass wool were used (app. 23% and 54% for bending strength and 68% and 72% for compressive strength). Use of the waste materials selected for the preparation of alternative activators might not be as promising as expected, since the concentration of Si in leachate is much lower than in commercial sodium silicate. When each of these waste-based activators are used in combination with precursors like slag, and then compared to the blank sample activated solely with NaOH (and not sodium silicates), an improvement in mechanical properties is seen. In future investigations, it is recommended to clarify the hardening mechanism of slag activated with alternative activators.

Declaration of competing interest

The authors declare that they have no known competing financial

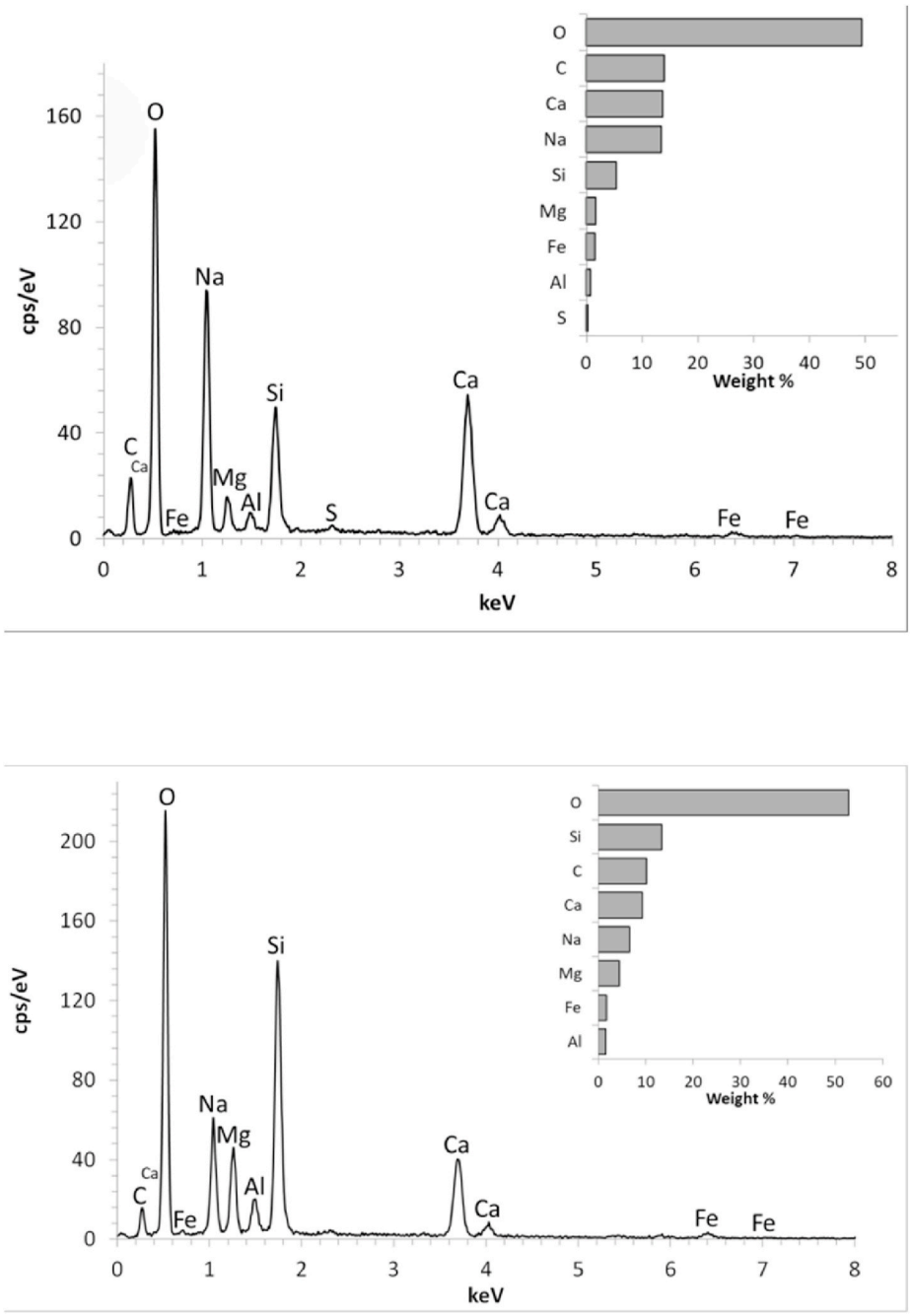

Fig. 7. EDS spectra of a) GWA-4h-SLAG and b) Ref-Water glass-SLAG.

interests or personal relationships that could have appeared to influence the work reported in this paper.

Acknowledgements

We acknowledge financial support from the Slovenian Research Agency, Slovenia, through project No. J2-9197: Synthesis and characterization of alkali activated foams based on different waste..

References

[1] W.K.W. Lee, J.S.J. van Deventer, Use of infrared spectroscopy to study geopolymerization of heterogeneous amorphous aluminosilicates, Langmuir 19 (2003) 8726–8734.
[2] F. Pacheco-Torgal, J.A. Labrincha, C. Leonelli, A. Palomo, P. Chindaprasirt (Eds.), Handbook of Alkali-Activated Cements, Mortars and Concretes, Elsevier, 2015.
[3] M. Jiang, X. Chen, F. Rajabipour, C.T. Hendrickson, Comparative life cycle assessment of conventional, glass powder, and alkali-activated slag concrete and mortar, J. Infrastruct. Syst. 20 (4) (2014).
[4] J.L. Provis, Alkali-activated materials, Cement Concr. Res. 114 (2018) 40–48.
[5] J.L. Provis, Geopolymers and other alkali-activated materials: why, how, and what? Mater. Struct. 47 (2014) 11–25.
[6] L.K. Turner, F.G. Collins, Carbon dioxide equivalent (CO_2-e) emissions: a comparison between geopolymer and OPC cement concrete, Construct. Build. Mater. 43 (6) (2013) 125–130.
[7] G. Habert, J.B. d'Espinose de Lacaillerie, N. Roussel, An environmental evaluation of geopolymer based concrete production: reviewing current research trends, J. Clean. Prod. 19 (11) (2011) 1229–1238.
[8] Y.W. Liu, C.J. Shi, Z.H. Zhang, N. Li, An overview on the reuse of waste glasses in alkali-activated materials, Resour. Conserv. Recycl. 144 (2019) 297–309.
[9] Y. Jiang, T.-C. Ling, K.H. Mo, C. Shi, A critical review of waste glass powder – multiple roles of utilization in cement-based materials and construction products, J. Environ. Manag. 242 (2019) 440–449.
[10] N. Toniolo, A.R. Boccaccini, Fly ash-based geopolymers containing added silicate waste, A review, Ceram. Int. 43 (2017) 14545–14551.

[11] M. Cyr, R. Idir, T. Poinot, Properties of inorganic polymer (geopolymer) mortars made of glass cullet, J. Mater. Sci. 47 (2012) 2782–2797.
[12] M. Torres-Carrasco, F. Puertas, Waste glass as a precursor in alkaline activation: chemical process and hydration products, Construct. Build. Mater. 139 (2017) 342–354.
[13] F. Puertas, M. Torres-Carrasco, Use of glass waste as an activator in the preparation of alkali-activated slag. Mechanical strength and paste characterisation, Cement Concr. Res. 57 (2014) 95–104.
[14] P. Duxson, J.L. Provis, G.C. Lukey, S.W. Mallicoat, W.M. Kriven, J.S. Van Deventer, Understanding the relationship between geopolymer composition, microstructure and mechanical properties, Colloid. Surface. Physicochem. Eng. Aspect. 269 (2005) 47–58.
[15] C. Bobirică, J.-H. Shim, J.-H. Pyeon, J.-Y. Park, Influence of waste glass on the microstructure and strength of inorganic polymers, Ceram. Int. 41 (2015) 13638–13649.
[16] R. Redden, N. Neithalath, Microstructure, strength, and moisture stability of alkali-activated glass powder-based binders, Cement Concr. Compos. 45 (2014) 46–56.
[17] G. Taveri, J. Tousek, E. Bernardo, N. Toniolo, A.R. Boccaccini, I. Dlouhy, Proving the role of boron in the structure of fly-ash/borosilicate glass based geopolymers, Mater. Lett. 200 (2017) 105–108.
[18] P. Kinnunen, Y. Yliniemi, B. Talling, M. Illikainen, Rockwool waste in fly ash geopolymer composites, J. Mater. Cycles Waste Manag. 19 (2017) 1220–1227.
[19] Y. Yliniemi, B. Walkley, J.L. Provis, P. Kinnunen, M. Illikainen, Influence of activator type on reaction kinetics, setting time, and compressive strength of alkali-activated mineral wools, J. Therm. Anal. Calorim. (2020).
[20] J. Yliniemi, P. Kinnunen, P. Karinkanta, M. Illikainen, Utilization of mineral wools as alkali-activated material precursor, Materials 9 (5) (2016) 312.
[21] J. Yliniemi, T. Luukkonen, A. Kaiser, M. Illikainen, Mineral wool waste-based geopolymers, IOP Conf. Ser. Earth Environ. Sci. 297 (2019), 01200.
[22] J. Yliniemi, B. Walkley, J.L. Provis, P. Kinnunen, M. Illikainen, Nanostructural evolution of alkali-activated mineral wools, Cement Concr. Compos. 106 (2020) 103472.
[23] M. Torres-Carrasco, C. Rodríguez-Puertas, M. del Mar Alonso, F. Puertas, Alkali-activated slag cements using waste glass as alternative activators- Rheological behavior, Bol. Soc. Espanola Ceram. Vidr. 54 (2015) 45–57.
[24] F. Puertas, M. Torres-Carrasco, M.M. Alonso, 4 - reuse of urban and industrial waste glass as a novel activator for alkali-activated slag cement pastes: a case study, in: Handbook of Alkali-Activated Cements, Mortars and Concretes, 2015, pp. 75–109.
[25] M. Torres-Carrasco, J.G. Palomo, F. Puertas, Sodium silicate solutions from dissolution of glass wastes. Statistical analysis, Mater. Construcción 6 (314) (2014).
[26] M. Torres-Carrasco, F. Puertas, Waste glass in the geopolymer preparation. Mechanical and microstructural characterisation, J. Clean. Prod. 90 (2015) 397–408.
[27] A. Bouchikhi, M. Benzerzour, N.E. Abriak, W. Maherzi, Y.M. Pajany, Waste glass reuse in geopolymer binder prepared with metakaolin, Acad. J. Civ. Eng. 37 (2) (2019) 539–544.
[28] M. Keawthun, S. Krachodnok, A. Chaisena, Conversion of waste glasses into sodium silicate, Int. J. Chem. Sci. 12 (1) (2014) 83–91.
[29] K.T. Tong, R. Vinai, M.N. Soutsos, Use of Vietnamese rice husk ash for the production of sodium silicate as the activator for alkali-activated binders, J. Clean. Prod. 201 (2018) 272–286.
[30] E. Kamseu, L.M. Beleuk à Moungam, M. Cannio, N. Billong, D. Chaysuwan, U. C. Melo, C. Leonelli, Substitution of sodium silicate with rice husk ash-NaOH solution in metakaolin based geopolymer cement concerning reduction in global warming, J. Clean. Prod. 142 (2017) 3050–3060.
[31] H.K. Tchakouté, C.H. Rüscher, S. Kong, E. Kamseu, C. Leonelli, Thermal behavior of metakaolin-based geopolymer cements using sodium waterglass from rice husk ash and waste glass as alternative activators, Waste Biomass Valorization 8 (2017) 573–584.
[32] K. Traven, K. König, M. Pavlin, V. Ducman, Report on Results of Project J2-9197, Internal Report, 2020.
[33] M. Češnovar, K. Traven, B. Horvat, V. Ducman, The potential of ladle slag and electric arc furnace slag use in synthesizing alkali activated materials; the influence of curing on mechanical properties, Materials 12 (7) (2019) 1173.
[34] B.H.W.S. de Jong, G.E. Brown, Polymerization of silicate and aluminate tetrahedra in glasses, melts and aqueous solutions—II. The network modifying effects of Mg2 + , K+, Na+, Li+, H+, OH−, F−, Cl−, H2O, CO2 and H3O+ on silicate polymers, Geochem. Cosmochim. Acta 44 (11) (1980) 1627–1642.
[35] E.H. Oelkers, S.R. Gislason, The mechanism, rates and consequences of basaltic glass dissolution: I. An experimental study of the dissolution rates of basaltic glass as a function of aqueous Al, Si and oxalic acid concentration at 25°C and pH = 3 and 11, Geochem. Cosmochim. Acta 65 (21) (2001) 3671–3681.
[36] E.M. Gartner, D.E. Macphee, A physico-chemical basis for novel cementitious binders, Cement Concr. Res. 41 (7) (2011) 736–749.
[37] H.A. Gasteiger, W.J. Frederick, R.C. Streisel, Solubility of aluminosilicates in alkaline solutions and a thermodynamic equilibrium model, Ind. Eng. Chem. Res. 31 (4) (1992) 1183–1190.
[38] K.C. Newlands, M. Foss, T. Matchei, J. Skibsted, D.E. Macphee, Early stage dissolution characteristics of aluminosilicate glasses with blast furnace slag- and fly-ash-like compositions, J. Am. Ceram. Soc. 100 (5) (2017) 1941–1955.
[39] C. Ruiz-Santaquiteria, M. Torres-Carrasco, M.M. Alonso, F. Puertas, Valorización de residuos vítreos en la elaboración de morteros alcalinos, Workshop on Environmental Impact of building Construction, Universidad Politécnica de Madrid, 2013.
[40] U. Rattanasak, P. Chindaprasirt, Influence of NaOH solution on the synthesis of fly ash geopolymer, Miner. Eng. 22 (2009) 1073–1078.